The oxidative addition and migratory 1,1-insertion in the Monsanto and Cativa processes. A density functional study of the catalytic carbonylation of methanol

ARTICLE *in* JOURNAL OF MOLECULAR STRUCTURE THEOCHEM · JUNE 2001

Impact Factor: 1.37 · DOI: 10.1016/S0166-1280(00)00859-9

ELSEVIER

Journal of Molecular Structure (Theochem) 542 (2001) 273–288

THEO CHEM

www.elsevier.nl/locate/theochem

The oxidative addition and migratory 1,1-insertion in the Monsanto and Cativa processes. A density functional study of the catalytic carbonylation of methanol

T. Kinnunen, K. Laasonen*

Department of Chemistry, University of Oulu, P.O Box 3000, FIN-90014 Oulu, Finland

Received 20 October 2000; revised 1 December 2000; accepted 6 December 2000

Abstract

Density functional theory with hybrid B3LYP exchange and correlation functional has been used to investigate the first two catalytic reactions, the oxidative addition and migratory 1,1-insertion of the Monsanto and Cativa processes. One of the main interests has been to study if the previously unidentified *trans* forms of the active catalytic species $[Rh(CO)_2I_2]^-$ (**1**) or $[Ir(CO)_2I_2]^-$ (**2**) have any significance in these processes. The oxidative addition has been studied using both *cis* and *trans* forms of **1** and **2**. We have also studied the oxidative addition of methyl iodide to $[Rh(CO)_2I_3]^{2-}$ (**3**). In addition, different isomers of dicarbonyls $[CH_3Rh(CO)_2I_3]^-$ (**4**) and $[CH_3Ir(CO)_2I_3]^-$ (**5**) and tricarbonyl $[CH_3Ir(CO)_3I_2]$ (**8**) has been used in the 1,1-insertion study to see if these could provide new, alternative reaction pathways. The calculated free energies of activation for the oxidative addition of methyl iodide to *cis*-**1** and *cis*-**2** are 20.8 and 16.9 kcal/mol, respectively. The corresponding free energy barriers for *trans*-**1** and *trans*-**2** are 15.0 and 13.2 kcal/mol, respectively. The oxidative addition is the rate-determining step in the Monsanto process and the reaction with *trans*-**1** is predicted to accelerate that step. The presence of **3** could enhance the addition even more; the free energy of activation is only 5.6 kcal/mol. For the 1,1-insertions we have found similar activation energies in *fac*,*cis*- and *mer*,*trans*-structures. In the rhodium system, the free energies of activation are in the order of 20 kcal/mol and in the iridium system 30 kcal/mol. Interestingly, the insertions in *mer*,*cis*-dicarbonyls have considerably lower activation energies, half of those calculated for the insertions in *mer*,*trans*- and *fac*,*cis*-structures. The iodide dissociation from *fac*,*cis*-**5** could provide the path to *mer*,*cis*-**5** and so significantly enhance the rate of the insertion in the iridium system. The rate of the insertion should also increase if experimentally proposed tricarbonyl **8** is used instead of **5**. According to our calculations of different isomers of **8**, this seem to be true although the insertion barrier in *mer*,*cis*-**5** is calculated to be even lower. Our results are consistent with the experiments and other computational results. These results show that the geometrical arrangement of the ligands has a very large effect on the catalytic activity of the complexes and this suggests possible improvements to these industrially important processes.

Keywords: Rhodium; Iridium; Catalysis; Carbonylation; Density functional theory

1. Introduction

The catalytic carbonylation of methanol by the Monsanto acetic acid process [1] is one of the most efficient procedures used to manufacture acetic acid industrially. The main advantages of the Monsanto

* Corresponding author. Tel.: +358-8-5531640; fax: +358-85-531-603.

E-mail addresses: tapani.kinnunen@oulu.fi (T. Kinnunen), kari.laasonen@oulu.fi (K. Laasonen).

0166-1280/01/$ - see front matter
PII: S0166-1280(00)00859-9

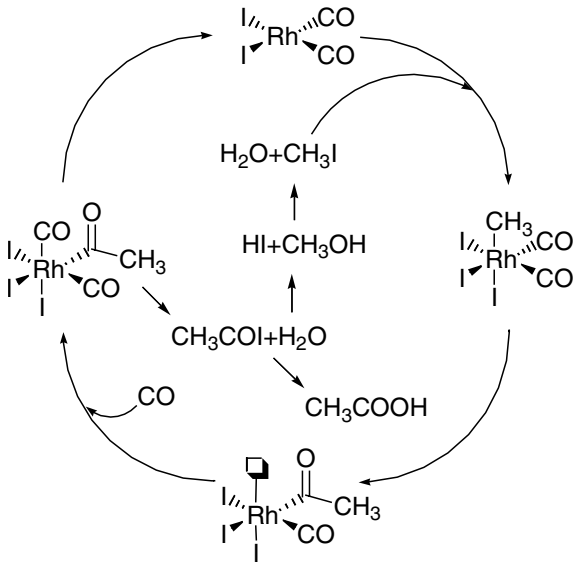

Fig. 1. Proposed mechanism for the Monsanto acetic acid process.

procedure are the low temperature and pressure needed. This process is studied widely experimentally and assumptions for the mechanisms, kinetics and thermodynamics of this process are available [2–6]. However, the computational studies on the topic are so far very few [7–9].

The active catalytic species in the process is a diiododicarbonylrhodate anion $[Rh(CO)_2I_2]^-$ that has been shown to be formed from various rhodium compounds and iodine promoters [10]. There is also a great interest in an analogous iridium system called the Cativa process [1,3,11]. This process is very similar to the rhodium system but shows even more enhanced rate and selectivity. The experiments have verified the existence and participation of the *cis* forms of the active species in the catalysis cycle. The actual catalysis cycles of the Monsanto and Cativa processes consist of a series of reactions including oxidative addition, 1,1-insertion, CO association and reductive elimination. The oxidative addition is the rate-determining step of the Monsanto process whereas in the Cativa process, the 1,1-insertion is the rate-determining step. Reaction cycles yield acetic acid with purity of 99.9 + % [12]. A proposed mechanism for the Monsanto process is illustrated in Fig. 1.

We have studied the catalytic carbonylation of methanol with ab initio methods. In our previous work [9] we concentrated on the active catalytic species $[Rh(CO)_2I_2]^-$ (**1**) and $[Ir(CO)_2I_2]^-$ (**2**). This study showed that *cis*-**1** has 4.9 kcal/mol lower free energy than *trans*-**1**, and *cis*-**2** has 10.4 kcal/mol lower free energy than *trans*-**2**. We found that the *cis* forms of the active species are nearly exactly square planar while the *trans* structures are twisted. In the previous study, we also investigated the mechanisms of the *cis* to *trans* isomerizations. The free energy barrier was 13.7 kcal/mol for the rhodium complex and 19.8 kcal/mol for iridium. According to these results, previously unidentified *trans* forms of the active species are possible and reasonable isomerization paths from the *cis* to *trans* catalysts exist. Therefore, in the current study we are interested to see if the *trans*-**1** or *trans*-**2** could play a role in the actual catalytic reactions. In this paper the first two reactions of the Monsanto and Cativa processes including the oxidative addition and 1,1-insertion have been studied. Both the *cis* and *trans* forms of the active catalytic species have been used as starting structures for the oxidative addition. The oxidative addition has been studied using 5-coordinated $[Rh(CO)_2I_3]^{2-}$ (**3**) as well. The schematic illustration of the starting structures *cis*-**1**, *cis*-**2**, *trans*-**1**, *trans*-**2** and **3** is presented in Fig. 2. The 1,1-insertion has been investigated using several possible reaction routes, including different isomers of dicarbonyl $[CH_3M(CO)_2I_3]^-$ (M = Rh, Ir) and neutral tricarbonyl $[CH_3Ir(CO)_3I_2]$.

The experimental data of these carbonylation processes consist of spectroscopic measurements that give information only on the dominant species present in the model systems. The intermediate structures of the catalysis cycles are short-lived species and the distribution of the different isomers depends strongly on the chemical history of the system. Thus, the dominant intermediates do not have to be thermodynamically the most stable or catalytically most active ones. Previous arguments give the motivation to study different isomers and reactions paths and to see if these could have any significance in the catalysis cycles. The previously unpublished reaction routes that the other theoretical groups have not calculated or the experimentalists have not been able to study, could propose some new enhancement possibilities for these processes. In addition, we believe that our results will verify the already known data from the *cis* systems.

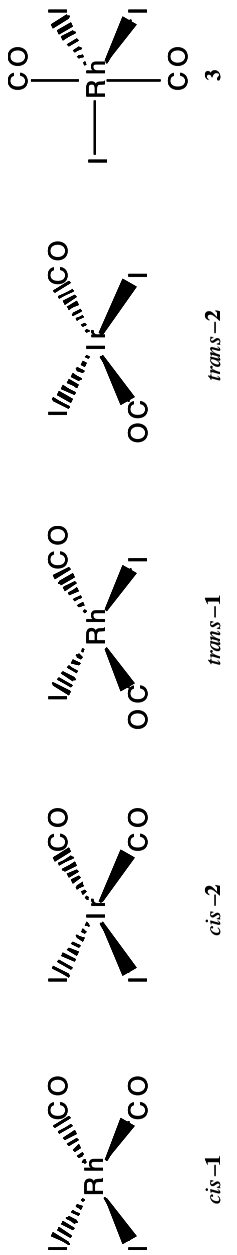

Fig. 2. The schematic illustrations of the starting structures *cis*-**1**, *cis*-**2**, *trans*-**1**, *trans*-**2** and **3**.

2. Computational details

As in our previous study [9], the density functional calculations have been based on the hybrid B3LYP [13,14] exchange and correlation (XC) functional and the GAUSSIAN 98 [15] program package. The basis set is denoted SDD and consists of a D95V for carbon, oxygen and hydrogen atoms. The Stuttgart/Dresden effective core potentials with scalar relativistic corrections have been used for rhodium, iridium and iodine. In our calculations, an extra fine integration grid has been employed. The methods that have been used here have worked well in studies of similar organometallic catalysis systems [16,17] and therefore we are confident that the computational scheme is adequate.

The Berny optimization algorithm has been used to obtain the minimum energy and transition state structures. First guess for the transition states has been determined with the Synchronous Transit-guided Quasi-Newton methods or potential energy surface (PES) scans. The PES has been scanned with a constrained optimization along a chosen reaction coordinate that has been a distance between two atoms.

The frequency analysis of the stationary points has been performed to verify the minimum energy and the transition state geometries. All the transition states have one imaginary frequency while the minimum energy structures have none. The frequency analyses have also given the approximation for the free energies by assuming rigid molecules and harmonic approximation to the vibrational states. The free energies that we report here have all been approximated at 298.15 K. Our studies have been performed in a gas phase and no symmetry constraints have been utilized. Due to quite large HOMO–LUMO gap, all structures have been calculated as singlet states.

3. Results and discussion

3.1. S_N2 type oxidative addition of CH_3I to $[M(CO)_2I_2]^-$ ($M = Rh, Ir$)

The first reaction in the catalysis cycle is an oxidative addition of methyl iodide to the active catalyst. The experimental studies [2,4] indicate the two-step S_N2 mechanism with a nucleophilic attack from the metal center with linear transition state and iodide as a leaving group. The iodide association in the *trans* position to the methyl group follows this. In the methyl iodide addition, the oxidation state of the metal center changes from I to III. In addition to the experimental proof, the S_N2 mechanism is confirmed in a brief Hartree–Fock computational study [7]. Oxidative addition is the rate-determining step in the rhodium system whereas in the iridium system, oxidative addition is fast and 1,1-insertion is the rate-determining step.

We have studied the oxidative addition of methyl iodide to *cis*-**1**, *trans*-**1**, *cis*-**2** and *trans*-**2**. At first we calculated reactant complexes where methyl iodide is in close proximity to the catalyst. These structures are from 4.8 kcal/mol (*trans*-**2** + methyl iodide) to 5.4 kcal/mol (*cis*-**1** + methyl iodide) lower in the potential energy when compared with the sum of the energies of catalyst and methyl iodide calculated at infinite separation.

Calculated transition states of the oxidative addition are presented in Fig. 3. While examining the transition state structures we can see that in the additions to *trans*-**1** or *trans*-**2**, the structure is linear. In the *cis*-systems, the methyl group and iodide tilt towards the carbonyls. The zero-point corrected potential energy barriers of the additions to *cis*-**1**, *trans*-**1**, *cis*-**2** and *trans*-**2** are 16.3, 10.4, 13.0 and 8.5 kcal/mol, respectively. The corresponding free energies of activation are 20.8, 15.0, 16.9 and 13.2 kcal/mol, so the negative activation entropies result in an increase of the activation energies by 3.9–4.7 kcal/mol. The calculated energetics of the oxidative additions is presented in Table 1. The experimental enthalpy barriers for the additions to the *cis*-$[M(CO)_2I_2]^-$ depend on the used solvent. For rhodium, the activation enthalpy [1,4] is 12–17 kcal/mol. The experimental free energy barrier [1,4] is 25.0 kcal/mol. The experimental activation enthalpy for the iridium [1] is 13.0 kcal/mol and corresponding free energy barrier is 21.0 kcal/mol. The calculated potential energy barriers for the *cis* systems match quite well with the experimental ones but the large negative entropies observed experimentally are underestimated. However, the calculated activation entropies are very similar in all additions studied and thus, we believe that the observed lower activation barriers to the *trans* forms are correct.

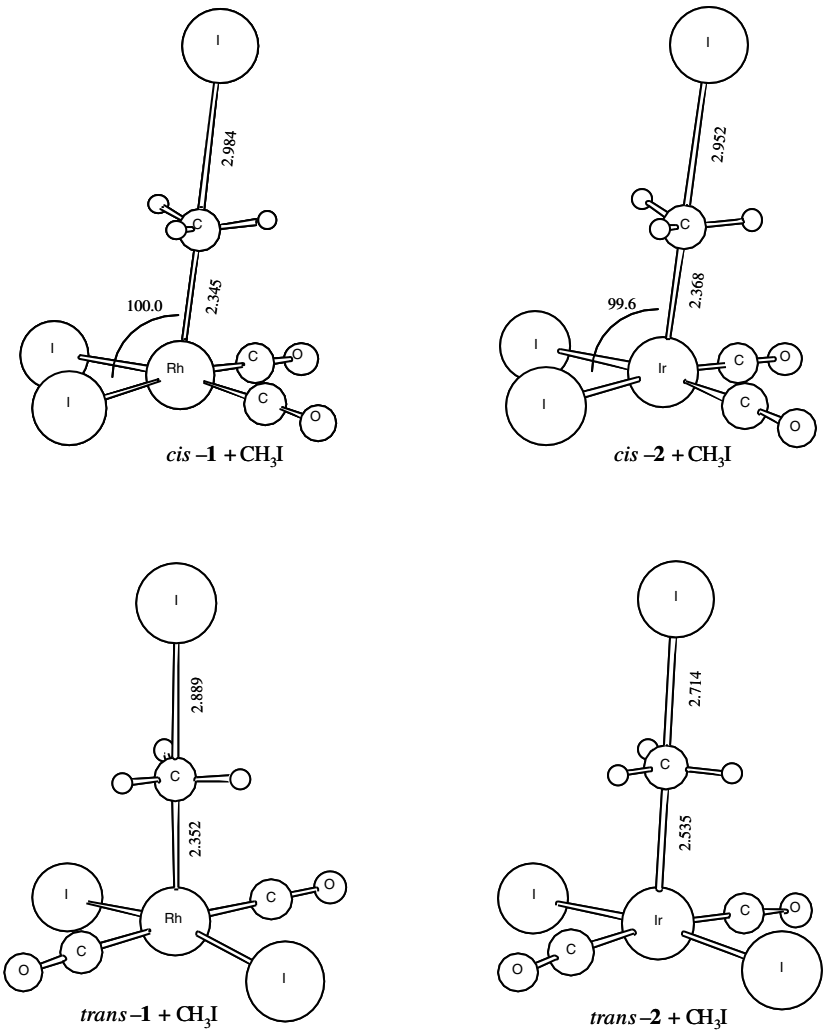

Fig. 3. Calculated transition states of the oxidative additions studied. Distances are given in Angstroms.

Table 1
Activation parameters and reaction energies of the different oxidative additions studied. The values are given in kcal/mol and total energy values include zero-point corrections. Superscript ‡ denotes for activation in the first step of the oxidative addition and R for reaction energy. Subscript add denotes for the first step of the oxidative addition and tot for total reaction energy of the addition. Experimental values are in parentheses if available. The energy differences are calculated by comparing with the corresponding reactant complex

Addition of CH_3I to	$\Delta E^{\ddagger}$	$\Delta G^{\ddagger}$	ΔE^{R}_{add}	ΔG^{R}_{add}	ΔE^{R}_{tot}	ΔG^{R}_{tot}
cis-**1**	16.3 (12–17) [1,4]	20.8 (~25) [1,4]	–	–	5.0	10.2
trans-**1**	10.4	15.0	–	–	−4.9	0.9
cis-**2**	13.0 (13.0) [1]	16.9 (21.0) [1]	–	–	−5.4	−1.3
trans-**2**	8.5	13.2	6.5	10.8	−16.6	−10.7
$[Rh(CO)_2I_3]^{2-}$	2.1	5.6	–	–	−55.6[a]	–

[a] Calculated as a sum of the energies of iodide and octahedral product complex.

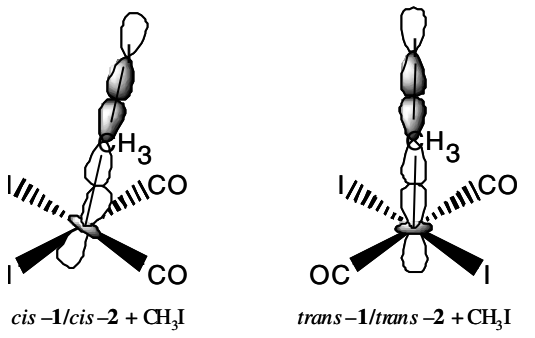

cis –**1**/*cis* –**2** + CH_3I *trans* –**1**/*trans* –**2** + CH_3I

Fig. 4. The schematic illustration of the interaction between the molecular orbitals in the transition states of the oxidative addition. The figure shows a clear difference between the *cis*- and *trans*-systems.

There is a trend between the activation barriers, M–C(methyl) distances and C(methyl)–I distances. The larger the barrier, the shorter M–C(methyl) distance and longer C(methyl)–I distance (Fig. 3), so when the barrier increases a "later" transition state respect to the M–C(methyl) distance is observed. The interesting point in the oxidative additions is that the activation barriers to previously unidentified *trans* systems are much lower than to experimentally verified *cis* systems and the iridium systems have smaller activation energies than rhodium systems.

To understand the difference between *cis* and *trans* systems, we have done some analysis of the molecular orbitals. The main interaction in the σ-type bonding in M–C(methyl) bond is the interaction between the metal d_z^2-orbital and C–I σ-orbital. This molecular orbital interaction is presented in Fig. 4 that shows the schematic illustration of the molecular orbitals of the transition states of the oxidative additions studied. In the plain catalysts **1** and **2**, the d_z^2-orbitals are orthogonal to the plane formed by the ligands. In the transition states of *trans* systems, CH_3I is located linearly on top of *trans*-**1** or *trans*-**2** and has a good overlap with the metal d_z^2-orbital. This results in "early" transition states and rather low activation barriers. When adding to *cis*-**1** or *cis*-**2**, CH_3I is not placed linearly and both the methyl group and iodide tilt towards to the carbonyls. The tilting is a consequence of the electrostatic repulsion between the iodide ligands and methyl iodide. The tilt causes the distortion of the metal d_z^2-orbital and raises the activation barriers in the *cis* systems. Due to a poorer overlap than in the *trans* systems, M–C(methyl) distances are shorter so the transition states in the *cis* systems are "later". The poorer overlap in *cis* systems can be verified by examining the 5-coordinated minimum energy structures $[CH_3M(CO)_2I_2]$ (M = Rh, Ir) where the iodide has been removed. In *cis* systems, the M–C(methyl) bonds are longer and therefore weaker than in the *trans* systems. This has also some effect on the relative stabilities of different structures. Due to weaker M–C(methyl) bonds the *cis* systems are less stable as before. In the case of rhodium the *trans* form has 3.7 kcal/mol lower free energy. In the iridium system after the methyl addition, the *cis* is still more stable but only by 0.4 kcal/mol.

The first step of the oxidative addition results in 5-coodinated $[CH_3M(CO)_2I_2]$ (M = Rh, Ir) and free iodide. We have put some effort into the study of the products of the first step and the iodide association. In the methyl iodide addition to *trans*-**2**, we have been able to locate a minimum energy stationary point where the iodide is in close proximity to the 5-coordinated product complex. The potential energy difference between the reactant complex and first product is 6.5 kcal/mol and the free energy difference is 10.8 kcal/mol, so here the first step is endothermic. In the case of the additions to *cis*-**1**, *trans*-**1** and *cis*-**2**, we have not been able to locate these minimum energy stationary points due to the problems caused by the iodide. When the C(methyl)–I distances approaches 3 Å, the modeling of iodide becomes difficult and causes convergence problems in the optimization. We have scanned the PES along M–I(associating) distance. These calculations indicate no activation barrier in the gas phase and easy iodide association leads to octahedral final product of the oxidative addition. These octahedral d^6-complexes will be discussed more precisely later in this paper. The overall reaction energies of the oxidative additions are presented in Table 1. Addition of methyl iodide to *cis*-**1** is endothermic and endergonic and to *trans*-**1** it is exothermic but slightly endergonic. The additions to iridium systems studied are both exothermic and exergonic. Our results here for the reaction energies of the additions to *cis*-**1** and *cis*-**2** follow the same trend that is observed with earlier HF-study [7].

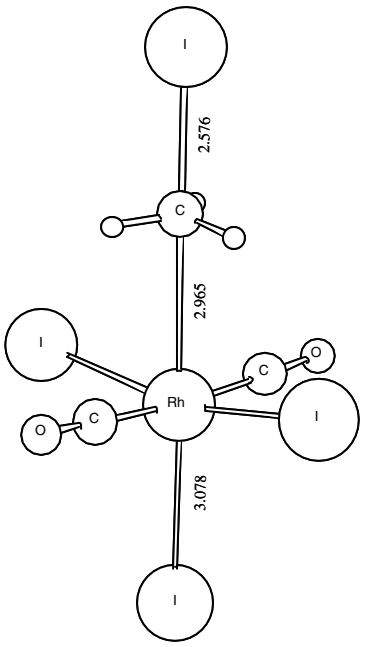

Fig. 5. Calculated transition state of the methyl iodide addition to 5-coordinated $[Rh(CO)_2I_3]^{2-}$ (**3**). Distances are given in Angstroms.

3.2. Methyl iodide addition to $[Rh(CO)_2I_3]^{2-}$ (*3*)

We have also studied the oxidative addition using more nucleophilic 5-coordinated $[Rh(CO)_2I_3]^{2-}$. There are suggestions [4] that this structure could be present in the experimentally studied systems. It is known [1], that high iodide concentration accelerates the reaction rate in the rhodium system, whereas in the iridium system high amount of iodide acts as an inhibitor. The effect of iodide concentration in the iridium system will be discussed later in this paper. The calculated structure of **3** has trigonal bipyramidal geometry with carbonyls in axial positions. We also studied the other possible isomers but during the structural optimization, they transformed back to the structure where carbonyls are in axial positions. The reactant complex, where CH_3I is in close proximity to **3**, is 10.6 kcal/mol in lower energy than truly separated molecules. The located linear and very "early" transition state of methyl iodide addition is presented in Fig. 5. The activation and reaction energies are presented in Table 1. The zero-point corrected potential energy barrier is only 2.1 kcal/mol and free energy barrier is 5.6 kcal/mol. Indeed, to this more nucleophilic species [18], the activation barrier of the addition is very small. While analyzing the molecular orbitals, it is interesting to see that the bonding of methyl group is different compared to the transition states of the additions to $[M(CO)_2I_2]^-$. Here the d_z^2-orbital has a bonding overlap with iodide *trans* to methyl. The methyl now interacts with $d_x^2 - y^2$-orbital. This process leads to octahedral $[CH_3Rh(CO)_2I_3]^-$ and free iodide, the total process being exothermic. However, we do not have estimation [9] to the activation energy of iodide association to the $[Rh(CO)_2I_2]^-$, so will not make any further conclusion of this system at this point.[1]

3.3. Octahedral key intermediates $[CH_3Rh(CO)_2I_3]^-$ (*4*) and $[CH_3Ir(CO)_2I_3]^-$ (*5*)

Octahedral d^6-complexes $[CH_3Rh(CO)_2I_3]^-$ (**4**) and $[CH_3Ir(CO)_2I_3]^-$ (**5**) are the products of the oxidative addition. The structures and behavior of these complexes are particularly interesting, since their existence was experimentally verified recently [5,6].

We have studied the three possible isomers of $[CH_3M(CO)_2I_3]^-$ (M = Rh, Ir). The calculated structures of *mer*,*trans*-**4**, *mer*,*cis*-**4**, *fac*,*cis*-**4**, *mer*,*trans*-**5**, *mer*,*cis*-**5** and *fac*,*cis*-**5** isomers of the octahedral d^6-complexes are presented in Fig. 6. The zero point corrected total energy differences show *mer*,*trans*-**4** to be the relatively most stable isomer in the rhodium system, *mer*,*cis*-**4** being 4.0 kcal/mol and *fac*,*cis*-**4** 3.9 kcal/mol higher in energy. The free energy differences show the same order in the relative stabilities, *mer*,*cis*-**4** being 4.4 kcal/mol and *fac*,*cis*-**4** 3.7 kcal/mol higher, respectively. In the iridium system *mer*,*trans*-**5** is relatively most stable, energy differences being smaller than in the rhodium system. Here *mer*,*cis*-**5** is 2.7 kcal/mol and *fac*,*cis*-**5** only 1.2 kcal/mol higher in zero-point corrected total energy. The free energy shows *mer*,*cis*-**5** to be 3.3 kcal/mol and *fac*,*cis*-**5** 1.8 kcal/mol higher in free energy. This data is shown in Table 2. Interesting point in *mer*,*trans*- and *fac*,*cis*-conformations of the structures **4** and **5** is that the energy difference between them is quite small, *mer*,*trans* structures

[1] This system will be studied more precisely in future.

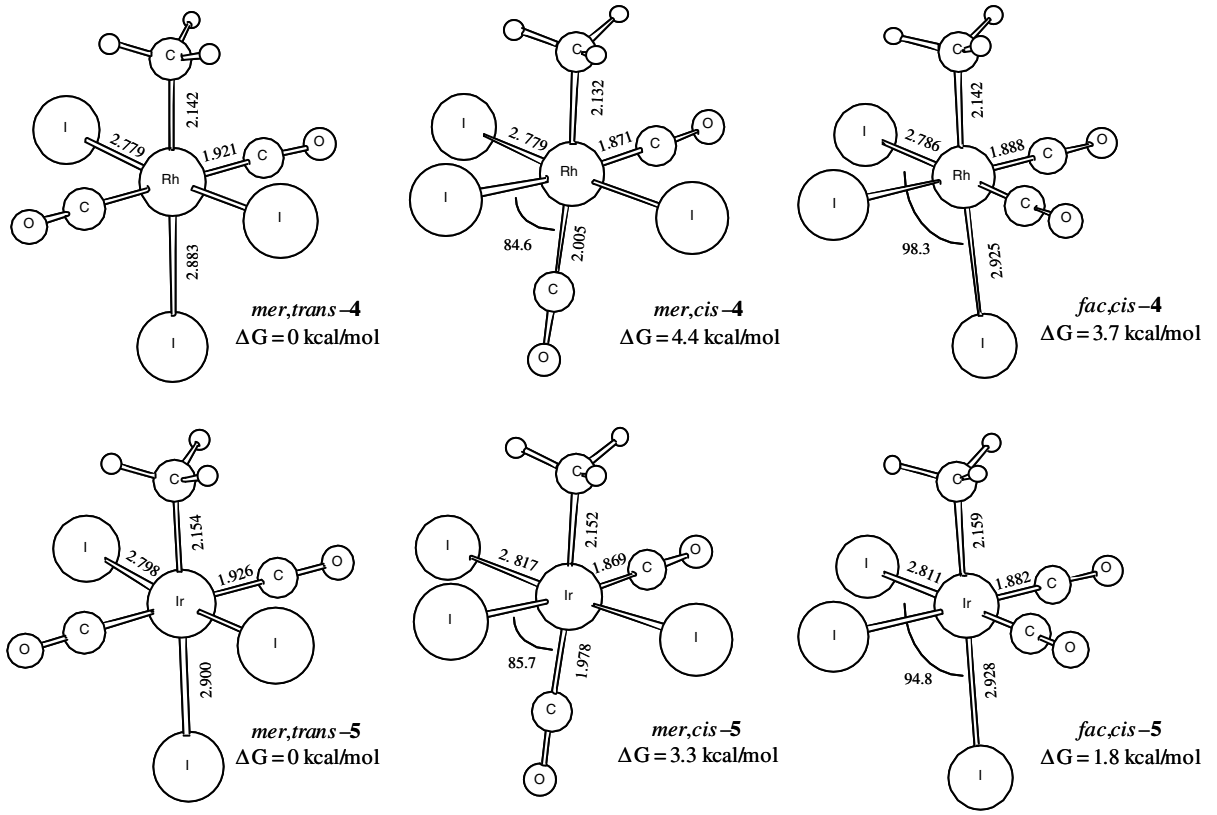

Fig. 6. Calculated minimum energy structures of the different isomers of dicarbonyls **4** and **5**. Distances are given in Angstroms. The relative free energies are calculated by comparing with *mer*,*trans*-isomers of **4** and **5**.

being in lower energy. This destabilization of the structure containing *cis*-fragment was already mentioned earlier, while checking structures $[CH_3M(CO)_2I_2]$ and the iodide addition seems to have even more destabilizing effect. In this case the destabilization of *fac*,*cis*-structures is probably due to the weaker M–I(*trans* to methyl) bonds than in *mer*,*trans*-structures (Fig. 6). Weaker bonds are due to the tilting of iodide towards the carbonyls, caused by the repulsion with other iodides. Our results show the *mer*,*cis*-structures of **4** and **5** to be the least stable of the different isomers. This can be explained with the weak M–C(carbonyl *trans* to methyl) bond (Fig. 6) that probably is caused by the *trans* influence of methyl group to carbonyl and by the slight tilting of the carbonyl towards the iodide-ligands.

Table 2
The calculated energy differences between different isomers of dicarbonyls $[CH_3Rh(CO)_2I_3]^-$ (**4**) and $[CH_3Ir(CO)_2I_3]^-$ (**5**). The values are given in kcal/mol and total energies include the zero-point correction. Energy differences are presented relative to *mer*,*trans*-**4** and *mer*,*trans*-**5**. The results calculated elsewhere are in parentheses for those systems where available

Species	ΔE	ΔG
mer,*trans*-**4**	0.0 (0.0) [8]	0.0
mer,*cis*-**4**	4.0 (0.6) [8]	4.4
fac,*cis*-**4**	3.9 (−0.3) [8]	3.7
mer,*trans*-**5**	0.0 (0.0) [8]	0.0
mer,*cis*-**5**	2.7 (0.1) [8]	3.3
fac,*cis*-**5**	1.2(−2.7) [8]	1.8

Our calculated results for structures **4** and **5** are qualitatively similar to those calculated by Cheong et al. [8]. There are small deviations in calculated relative stabilities but this is most probably due to difference in methods and programs used. We have tested the Gaussian results against some other ab initio programs using several XC-functionals and the

agreement is very good. Because the energy differences of the different structures are small, the deviations in the relative stabilities are understandable.

There is experimental IR- and NMR-data [5,6] for species **4** and **5**. The NMR-data indicates the presence of two equivalent carbonyls which is consistent with *fac*,*cis*- and *mer*,*trans*-species. The IR-data shows two CO-stretching modes of similar intensity, verifying the existence of *fac*,*cis*-structures. We have calculated the vibrational frequencies of the different isomers of **4** and **5**. The calculated CO-stretching modes and their intensities are given in Table 3. Our results show two carbonyl-stretching modes of similar intensity for *fac*,*cis*-**4** and *fac*,*cis*-**5**, results being consistent with the experiments. For *mer*,*trans*-structures, we also have two CO modes. Here the symmetric CO stretches have very low intensities and for both rhodium and iridium system the more intensive antisymmetric modes overlap with the antisymmetric modes of *fac*,*cis*-structures. According to this data, in addition to *fac*,*cis*-structures, *mer*,*trans*-structures could be present but only in rather low concentrations. The calculated CO-stretching modes for *mer*,*cis*-species are very similar to those of *fac*,*cis*-structures. So according to the IR-data, *mer*,*cis*-structures could also be present but they have not been observed with the NMR [5,6].

Overall, the spectroscopic methods can only isolate the dominating species that do not need to be the catalytically important ones. As in the case here, the experimentally unobserved species are catalytically much more active than the observed ones.

3.4. Migratory 1,1-insertion in $[CH_3Rh(CO)_2I_3]^-$ (4) or $[CH_3Ir(CO)_2I_3]^-$ (5)

The second reaction in the Monsanto and Cativa processes is 1,1-insertion that goes via intramolecular methyl migration to carbonyl ligand. This reaction is studied experimentally [1,5,6] and insertion in the *fac*,*cis*-structures is proposed. There is also a computational Density functional study [8] with BP86 XC-functional including the insertions in experimentally proposed *fac*,*cis*-structures. In the rhodium system, this reaction is fast while in the iridium system it is shown to be the rate-determining step. In addition to the new reaction routes that we now have studied, we also compare our results with those routes calculated by Cheong et al. [8] for *fac*,*cis*-structures.

Table 3
The calculated wave numbers (cm^{-1}) of the CO-stretching modes for the different isomers of **4** and **5**. The intensities of the modes are given in parentheses

CO-mode	ν_1	ν_2
mer,*trans*-**4**	1979.2 (1175)	2039.8 (23)
mer,*cis*-**4**	1973.0 (557)	2008.1 (477)
fac,*cis*-**4**	1973.6 (430)	2010.8 (639)
mer,*trans*-**5**	1964.5 (1342)	2045.4 (20)
mer,*cis*-**5**	1960.7 (664)	2008.1 (525)
fac,*cis*-**5**	1964.7 (545)	2014.8 (664)

The transition states of the intramolecular 1,1-insertions in the different isomers of **4** and **5** studied are presented in Fig. 7. The transition states are all very similar, methyl migrating towards the carbonyl. In the transition states for insertions in *mer*,*cis*- and *fac*,*cis*-structures the iodide *trans* to reacting carbonyl has moved slightly towards the migrating methyl group. The zero-point corrected potential energy barriers of the 1,1-insertions in *mer*,*trans*-**4**, *mer*,*cis*-**4**, *fac*,*cis*-**4**, *mer*,*trans*-**5**, *mer*,*cis*-**5** and *fac*,*cis*-**5** are 19.5, 10.3, 17.9, 28.8, 15.7 and 28.1 kcal/mol, respectively. The corresponding free energy barriers are 20.5, 11.1, 19.2, 30.2, 16.6 and 28.8 kcal/mol. In 1,1-insertion, the negative entropies of activation raise the barriers. The calculated activation energies are presented in Table 4. The experimental activation enthalpy [6] for the rhodium system is 15.0 kcal/mol and the activation enthalpy calculated by Cheong et al. [8] is 18.7 kcal/mol. The corresponding free energy barriers [6,8] are 19.3 kcal/mol and 18.4 kcal/mol. For the iridium system, the experimental activation enthalpy [20] is 37.0 kcal/mol and that computed by Cheong et al. [8] is 29.8 kcal/mol. The corresponding free energies of activation [8,20] are 30.6 and 29.2 kcal/mol. Our results for insertion in *fac*,*cis*-**4** are quite good compared with the experimental and results by Cheong et al.. One deficiency in computational results seems to be the calculated insertion in *fac*,*cis*-**5**. In this case either our static calculations or the static calculations made by Cheong et al. [8] have not been able to predict the experimental activation enthalpy and the activation entropy. It is proposed [8] that this is connected to the entropy

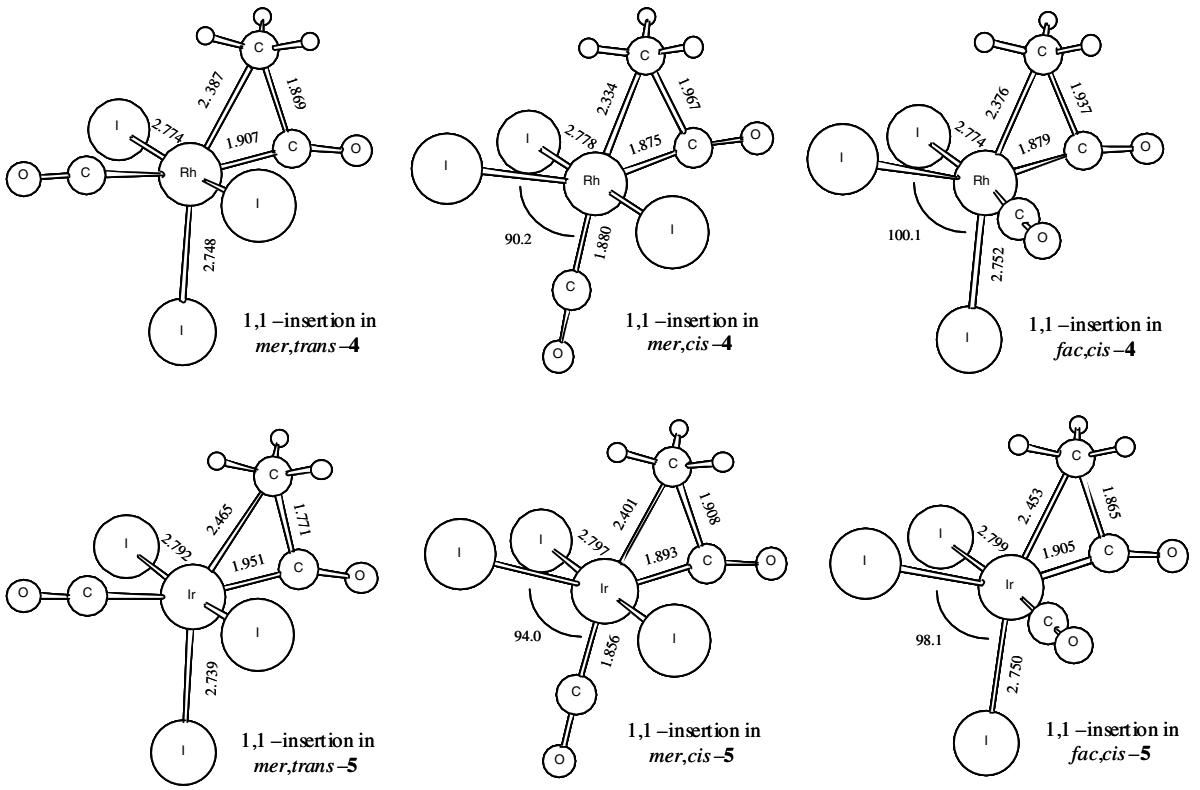

Fig. 7. Calculated transition states of the migratory 1,1-insertions in different isomers of **4** and **5**. Distances are given in Angstroms.

favored iodide dissociation from *fac*,*cis*-**5** occurring at the same time that the insertion takes place. It seems that this phenomenon cannot be modeled correctly by the static calculations.

The activation energies of the 1,1-insertions in the iridium system are higher than the corresponding activation energies in the rhodium system, so the 1,1-insertions are slower in the iridium system. The insertions in *mer*,*trans*- and *fac*,*cis*-structures have very similar activation energies, differences being within a few kilocalories per mole. Our results from the insertions in *mer*,*cis*-structures are very interesting.

Table 4
Activation parameters and reaction energies of the different 1,1-insertions studied. The values are given in kcal/mol and total energy values include zero-point corrections. Superscript ‡ denotes for activation parameters and R for reaction energy. Experimental and elsewhere calculated values are in parentheses if available

Insertion in	$\Delta E^{\ddagger}$	$\Delta G^{\ddagger}$	ΔE^{R}	ΔG^{R}
mer,*trans*-**4**	19.5	20.5	15.0	15.2
mer,*cis*-**4**	10.3	11.1	−11.2	−11.0
fac,*cis*-**4**	17.9 (15.0[a], 18.7[b]) [6,8]	19.2 (19.3[a], 18.4[b]) [6,8]	−11.1 (−8.84[a],−6.13[b]) [6,8]	−10.3 (−5.00[a],−6.81[b]) [6,8]
mer,*trans*-**5**	28.8	30.2	27.4	27.9
mer,*cis*-**5**	15.7	16.6	−4.0	−3.8
fac,*cis*-**5**	28.1 (37.0[a], 29.8[b]) [20,8]	28.8 (30.6[a], 29.2[b]) [20,8]	−2.6 (3.54[b]) [8]	−2.3 (2.46[b]) [8]

[a] Experimental.
[b] Computational.

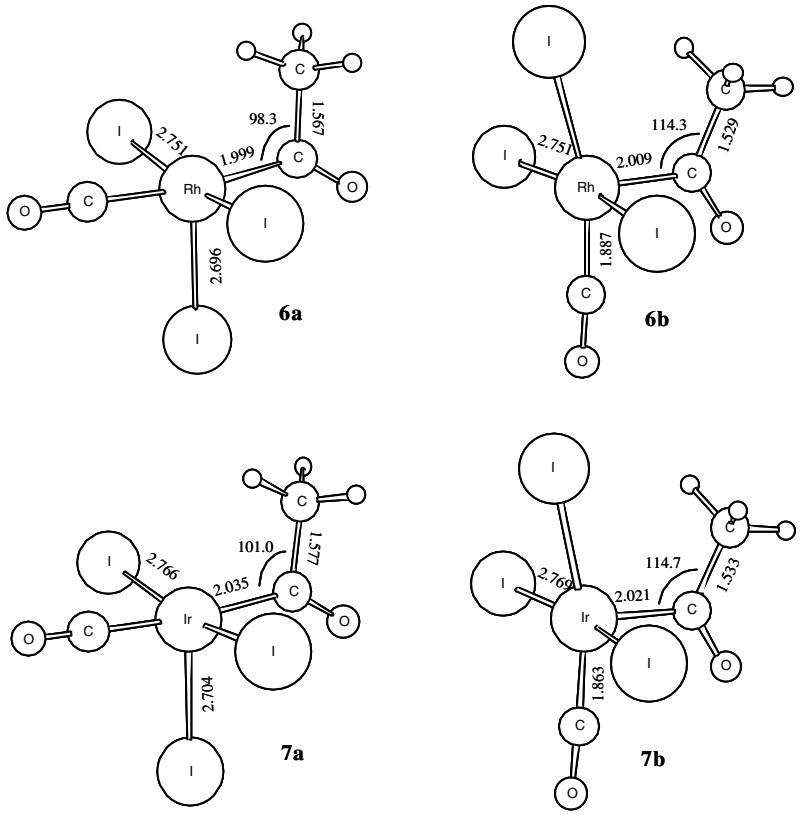

Fig. 8. The different conformations of the acyl complexes **6** and **7** formed via the 1,1-insertion. Distances are given in Angstroms.

Activation energy for the insertions in these systems are only about half of those predicted for *mer*,*trans*- or *fac*,*cis*-systems. This is probably due to the well-known *trans* effect. In this case the *trans* effect of the carbonyl to migrating methyl lowers the energy of the transition state of the insertion. The lower activation energy of the insertions in *mer*,*cis*-systems could provide enhanced rate for this reaction which would be important especially in the iridium system. There is some experimental evidence [19] indicating that *mer*,*cis*-species are not possible direct products of the oxidative addition, and therefore we have been interested to see if one could transform *mer*,*trans*- or *fac*,*cis*-species to *mer*,*cis*-species. This transformation could be achieved by dissociating one of the carbonyl ligands from the octahedral structures, because the remaining 5-coordinated structures are expected to be very fluxional. The carbonyl dissociation in low carbon monoxide pressure has been observed experimentally for the rhodium system [21]. We have done some calculations of the carbonyl dissociation. For the carbonyl dissociation from *mer*,*trans*-**4**, *fac*,*cis*-**4**, *mer*,*trans*-**5** and *fac*,*cis*-**5** the calculated zero-point corrected potential energy barriers are 29.1, 29.2, 34.4 and 39.6 kcal/mol, respectively. The activation entropies for these processes are slightly positive and the free energy barriers are 28.6, 28.8, 34.1 and 38.4 kcal/mol, respectively. The calculated activation parameters for carbonyl dissociations from different species are higher than for the corresponding insertions, so the CO-dissociations from *mer*,*trans*- or *fac*,*cis*-species seem unlikely. The iodide dissociation will be discussed later.

The 1,1-insertions studied lead to 5-coordinated square-pyramidal d^6-acyl complexes $[Rh(CO)(CO\text{-}CH_3)I_3]^-$ (**6**) and $[Ir(CO)(COCH_3)I_3]^-$ (**7**) with a vacant coordination site. The acyl complexes are presented in Fig. 8. The insertions in *mer*,*trans*-**4** and *mer*,*trans*-**5** result in the structures **6a** and **7a**,

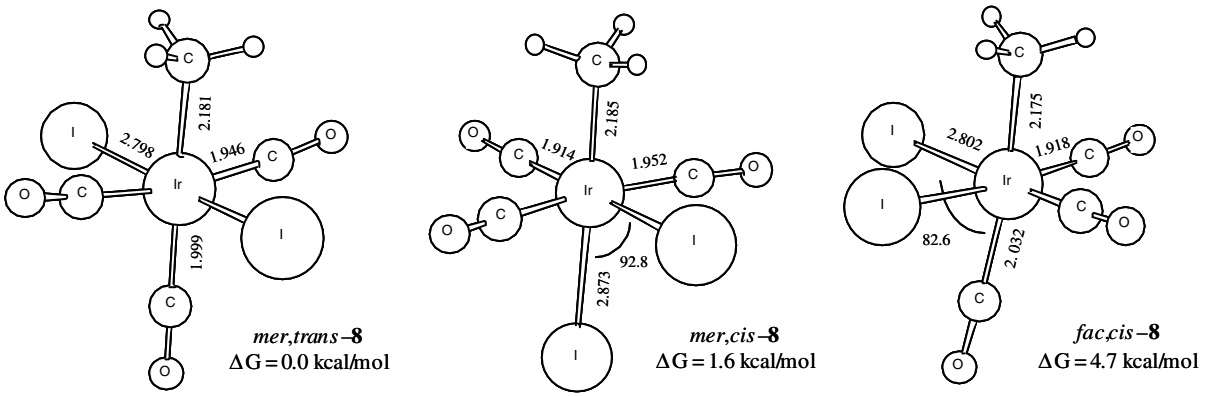

Fig. 9. Calculated minimum energy structures of different conformations of neutral tricarbonyl $[CH_3Ir(CO)_3I_2]$ (**8**). Distances are given in Angstroms. The relative free energies are calculated by comparing with *mer*,*trans*-**8**.

where iodide is in the apical position, while insertions in *mer*,*cis*- and *fac*,*cis*-systems lead to the same product, **6b** in rhodium and **7b** in iridium. These have the acyl group in apical position. The reaction energies of the insertions studied are shown in Table 4. Our results show the insertions in *mer*,*trans*-systems to be endothermic and endergonic. All the other insertions are exothermic and exergonic. The reaction energies seem to correlate with the structures of **6** and **7**. In structures **6a** and **7a**, the relative instability is due to an unfavorable orientation of the acyl group (Fig. 8). Our results for the reaction energies in *fac*,*cis*-**4** is consistent with the experiments [6] while small deviations with the results calculated by Cheong et al. [8] exist (Table 4). The differences in the computed reaction energies arise from differences in calculated relative stabilities of octahedral structures discussed earlier.

3.5. Migratory insertion in tricarbonyl complex $[CH_3Ir(CO)_3I_2]^-$ (8)

The experiments [3,11,22] show that enhanced rate for the insertion in the iridium system can be achieved via the neutral tricarbonyl complex $[CH_3Ir(CO)_3I_2]$ (**8**). The formation of **8** starts with iodide dissociation from the octahedral dicarbonyl complexes that were discussed earlier. The resulting 5-coordinated intermediate complex form a dimer that reacts with carbonyl yielding the tricarbonyl $[CH_3Ir(CO)_3I_2]$. This is considered the reason why iodide acts as an inhibitor in the iridium system; high iodide concentration slows down the iodide dissociation and reduces the amount of tricarbonyl in the system and thus slows down the total reaction rate. The tricarbonyl complexes and the insertions in them have already been studied computationally by Cheong et al. [8]. For comparison, we will briefly present our results from these systems.

We have done the PES scans to see if the iodide ligand could be removed from the octahedral *mer*,*trans*- or *fac*,*cis*-dicarbonyls. These calculations show that the only iodides that can be removed are the iodides in *fac*,*cis*-**5**. From these, removal of the iodide *trans* to the methyl group seems to be easier. All the other iodide dissociations from *mer*,*trans*- or *fac*,*cis*-isomers of the structures **4** and **5** have larger activation barriers than do the migratory insertions. This supports the proposition [8] that iodide could dissociate from *fac*,*cis*-**5** during the insertion. Our conclusions of iodide dissociation are similar to those predicted by Cheong et al. with CP-PAW molecular dynamics simulation [8]. It is proposed that iodide dissociation could also lead to isomerization [8] in the iridium system. In addition to different forms of tricarbonyl $[CH_3Ir(CO)_3I_2]$, we think that by capture of the iodide-ligand instead of CO, the isomerization could lead to dicarbonyl such as *mer*,*cis*-**5** that would enhance the insertion rate in the iridium system.

The different isomers *mer*,*trans*-**8**, *mer*,*cis*-**8** and *fac*,*cis*-**8** of the tricarbonyl $[CH_3Ir(CO)_3I_2]$ are presented in Fig. 9. The calculated relative stabilities of the different isomers are shown in Table 5, showing the *mer*,*trans*-**8** being the relatively most stable isomer, although *mer*,*cis*-**8** is only marginally less

Table 5
The calculated energy differences between different isomers of tricarbonyl $[CH_3Ir(CO)_3I_2]$ (**8**). The values are given in kcal/mol and total energies include the zero-point correction. Energy differences are presented relative to *mer*,*trans*-**8**. The results calculated elsewhere are in parentheses

Species	ΔE	ΔG
mer,*trans*-**8**	0.0	0.0 (0.0) [8]
mer,*cis*-**8**	1.4	1.6 (−0.3) [8]
fac,*cis*-**8**	4.4	4.7(0.7) [8]

Table 6
The calculated wave numbers (cm^{-1}) of the CO-stretching modes for the different isomers of **8**. The intensities of the modes are given in parentheses

CO-mode	ν_1	ν_2	ν_3
mer,*trans*-**8**	2033.1 (1058)	2034.8 (491)	2099.9 (10)
mer,*cis*-**8**	2030.3 (512)	2035.0 (1034)	2096.9 (92)
fac,*cis*-**8**	2018.3 (478)	2030.8 (539)	2074.8 (499)

stable. Again, there are slight differences in the relative stabilities of the minimum energy structures, while comparing to the results calculated by Cheong et al. [8].

The experimental IR-data [22] shows three CO-stretches, all with similar intensity and consistent with *fac*,*cis*-geometry. The *trans* position of the extra carbonyl is verified with ^{13}C substitution. We have calculated the vibrational frequencies for different isomers of **8**. The CO-stretching modes and their intensities are in Table 6. Our result for *fac*,*cis*-**8** show three CO-stretching modes with similar intensity which is consistent with the experiments. According to the IR-data, significant concentrations of *mer*,*trans*-**8** and *mer*,*cis*-**8** should be observable in IR-spectrum, if present in the system; the two lower wave number modes of *mer*,*trans*-**8** and *mer*,*cis*-**8** would overlap with one of the CO-modes of *fac*,*cis*-**8** which would increase the intensity of that mode significantly. The experiments do not support *mer*,*trans*-**8** and *mer*,*cis*-**8**, but small concentrations of these species cannot be ruled out.

The calculated transition states for the insertions in the different isomers of **8** are presented in Fig. 10. The transition states have similar features compared to the dicarbonyls. In the *fac*,*cis*-system the iodide moves toward the migrating carbonyl. In the case *mer*,*cis*-**8**, two possible pathways for insertion is possible. We find the path where methyl migrates towards the carbonyl that is in trans position to other carbonyl more feasible. The zero-point corrected potential energy barriers for the insertions in *mer*,*trans*-**8**, *mer*,*cis*-**8** and *fac*,*cis*-**8** are 19.9, 26.7 and 19.8 kcal/mol, respectively. The corresponding free energy barriers are 20.8, 27.5 and 20.6 kcal/mol. This data is shown in Table 7. Our results in the case of the insertions in the tricarbonyl $[CH_3Ir(CO)_3I_2]$ are consistent with the available experimental data for *fac*,*cis*-**8** [22] and computational results by Cheong et al. [8] (Table 7).

The activation parameters show that the insertion in the iridium system is enhanced by the tricarbonyl

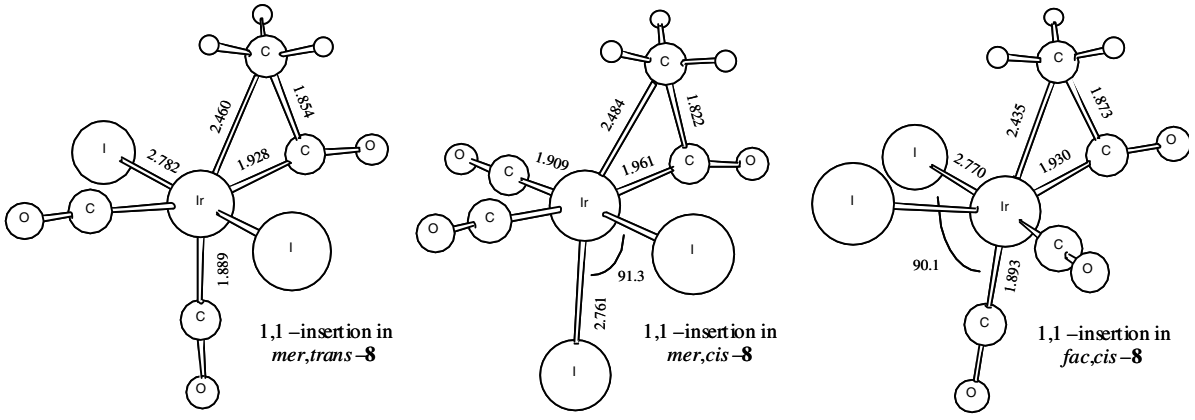

Fig. 10. Calculated transition states of the migratory 1,1-insertions in different isomers of **8**. Distances are given in Angstroms.

Table 7
Activation parameters and reaction energies of the 1,1-insertion studied in tricarbonyl $[CH_3Ir(CO)_3I_2]$ (**8**). The values are given in kcal/mol and total energy values include zero-point corrections. Superscript ‡ denotes for activation and R for reaction energy. Experimental values and values calculated elsewhere are in parentheses if available

Insertion in	$\Delta E^{\ddagger}$	$\Delta G^{\ddagger}$	ΔE^{R}	ΔG^{R}
mer,*trans*-**8**	19.9 (18.4[a]) [8]	20.8 (18.5[a]) [8]	15.3	15.1
mer,*cis*-**8**	26.7 (25.2[b]) [8]	27.5 (26.5[b]) [8]	21.8	21.5
fac,*cis*-**8**	19.8 (21.3[b], 18.7[a])[22,8]	20.6 (23.8[b], 19.8[a])[22,8]	−7.0 (−2.9[a]) [8]	−7.4 (−4.3[a]) [8]

[a] Experimental.
[b] Computational.

$[CH_3Ir(CO)_3I_2]$. The lower activation parameters are due to *trans* effect of carbonyl to methyl group. This is supported by the result from *mer*,*cis*-system; activation barrier is higher when there is iodide *trans* to methyl group. It is proposed that in general the more back-bonding ligands such as carbonyls are present, the more enhanced is the insertion rate [1]. However, as our results for the insertions in dicarbonyls *mer*,*cis*-**4** and *mer*,*cis*-**5** have shown, two carbonyls are sufficient to enhance the insertion significantly if the carbonyls are geometrically positioned correctly.

The 1,1-insertions in the tricarbonyl $[CH_3Ir(CO)_3I_2]$ lead to 5-coordinated acyl complexes $[Ir(CO)_2(CO\text{-}CH_3)I_2]$ (**9**) with a vacant coordination site. The acyl complexes are presented in Fig. 11. The insertions in *mer*,*trans*-**8**, *mer*,*cis*-**8** and *fac*,*cis*-**8** result in acyl complexes **9a**, **9b** and **9c**, respectively, all having a different ligand in apical position. In **9a** it is CO, in **9b** it is iodide and in **9c** it is the acyl group. The calculated reaction energies are presented in Table 7 showing the insertion in *fac*,*cis*-**8** to be exothermic and exergonic. The insertions in *mer*,*trans*-**8** and *fac*,*cis*-**8** are endothermic and endergonic which is, like in the case of the dicarbonyls *mer*,*trans*-**4** and *mer*,*trans*-**5**, due to the unfavorable orientations of the acyl group.

4. Conclusion

We have studied the first two reactions of the Monsanto and Cativa processes including the oxidative addition and migratory 1,1-insertion. In addition to the experimentally suggested reaction routes via the *cis* forms of the active catalyst $[M(CO)_2I_2]^-$ (M = Rh, Ir) we have studied some new possible reaction pathways. We have been particularly interested if experimentally unidentified *trans* forms of the active catalytic species and their derivatives could play a key role in these processes. Our results for the *cis* systems are consistent with the experimental findings from oxidative addition and 1,1 insertion. For the migratory insertions in *fac*,*cis*-dicarbonyl systems and $[CH_3Ir(CO)_3I_2]$-tricarbonyl systems, our results

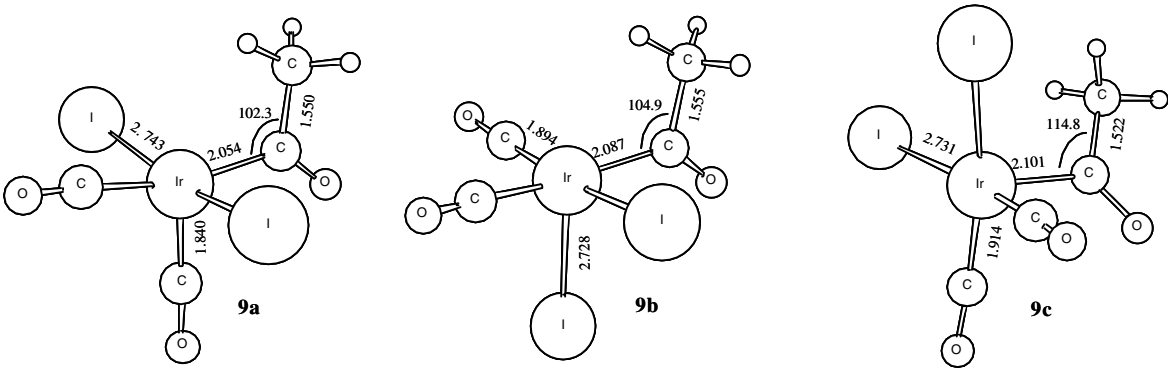

Fig. 11. The different forms of acyl complex **9** formed via the 1,1-insertion. Distances are given in Angstroms.

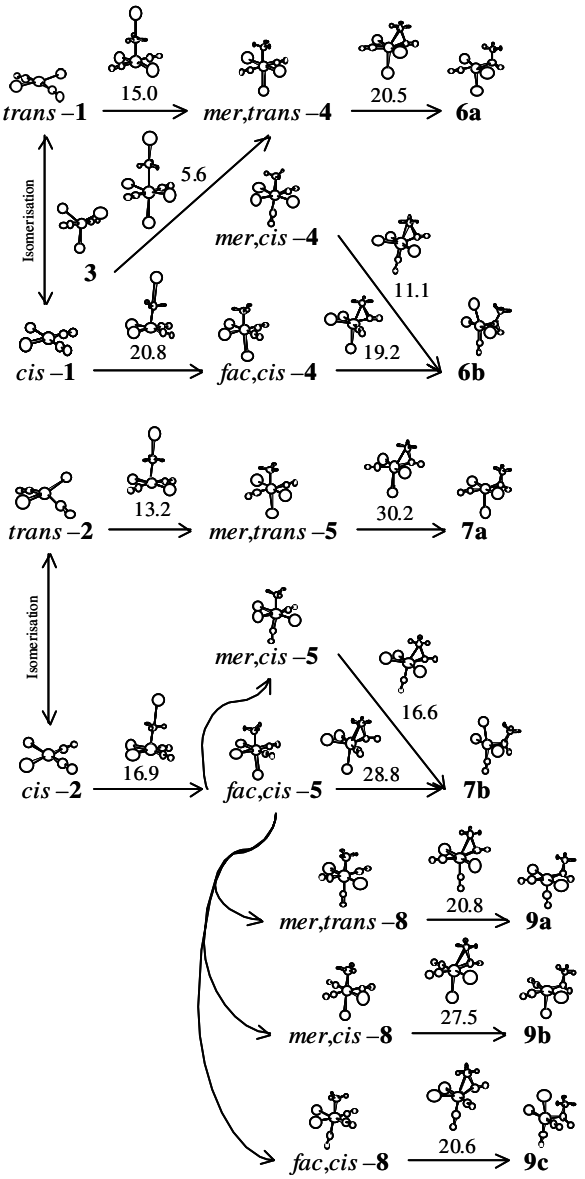

Fig. 12. The overall scheme of the different possible structures and reaction routes studied in the rhodium and iridium systems. An arrow indicates that the corresponding process is expected to occur. Missing arrow between two structures indicates that there is no knowledge if or how the transformation takes place. Numbers shown are the calculated free energy barriers in kcal/mol for the corresponding processes.

are consistent with the results calculated by Cheong et al. [8]. Small deviations in the computational results arise from different programs and methods used. We believe that our results and their trends from newly studied reaction pathways via *trans*-**1** or *trans*-**2** and other previously unreported results are reliable. The illustration of the different possible structures and reaction routes studied in the rhodium and iridium systems including the calculated free energies of activation is presented in Fig. 12.

For rhodium system we found the activation energy of the oxidative addition to *trans*-**1** is smaller than to *cis*-**1** and reaction with *trans*-**1** is exothermic and only slightly endergonic. The studies of 1,1-insertion show that activation energies of the insertion in *mer*,*trans*-**4** and *fac*,*cis*-**4** are about the same. In our previous study [9] we showed that in the rhodium system, the *trans* catalyst is a possible structure. According to results here, we propose that by the *trans*-**1**, the rate of catalytic cycle could rise because the oxidative addition via *cis* catalyst is the rate-determining step of the rhodium system and the insertion in *mer*,*trans*-**4** seems to be possible. The disadvantage of the *trans* path could arise from endothermic nature of 1,1-insertion in *mer*,*trans*-**4**. The next step in the Monsanto process is carbonyl association to a vacant coordination site of the acyl complex. This step is suggested to be very fast and therefore the catalysis cycle could still proceed through the insertion in *mer*,*trans*-**4**. Our results also reveal much lower activation energy for insertion in *mer*,*cis*-**4**. This would be a major enhancement for the insertion in the rhodium system but both carbonyl and iodide dissociations from *mer*,*trans*-**4** and *fac*,*cis*-**4** seem to be unlikely. In addition, our results show that even lower activation energy for oxidative addition is achieved with 5-coordinated $[Rh(CO)_2I_3]^{2-}$. This reflects the effect of nucleophilicity of the metal center to addition rate but this system needs more precise study [19].

For the iridium system, we found similar results as for the rhodium. The oxidative addition could be enhanced via *trans*-**2**. The insertion in *mer*,*trans*-**5** has about the same activation barrier as in *fac*,*cis*-**5**. Our previous study [9] has shown that the *trans* form of the active iridium catalyst is less likely and overall, the *trans* path would not be very significant in the iridium system because the insertion is the rate-determining step of the cycle and is not enhanced.

However, as in the rhodium system, the insertion in *mer*,*cis*-structure has much lower activation barrier and could provide much easier insertion in the iridium system. The carbonyl dissociation from *mer*,*trans*-**5** and *fac*,*cis*-**5** seem unlikely but as the experiments suggest, the iodide dissociation from *fac*,*cis*-**5** is possible. In addition to the tricarbonyl **8**, the iodide dissociation could provide path to *mer*,*cis*-**5** and so enhance the insertion rate. The insertions in the tricarbonyl **8** show, as the experiments suggest, that the activation barriers are lowered when compared to activation barriers of the insertion to *mer*,*trans*-**5** and *fac*,*cis*-**5**. However, it seems that two carbonyls are sufficient to enhance the insertion rates significantly if positioned correctly as in *mer*,*cis*-**5** where the insertion barrier is calculated to be even lower than in the tricarbonyls.

To conclude, we have showed some new structures and reaction route possibilities for the catalytic carbonylation of methanol that previously have not been considered. These results show that the geometrical arrangement of the ligands has very large effect on the catalytic activity of the complexes. We hope that these results will provide some guidance to the experimentalists as to the kind of structures and reaction paths that could provide improvements to these industrially important processes.

Acknowledgements

This work has been financed by Graduate School of Computational Chemistry and Molecular Spectroscopy. The authors would like to thank The Finnish Center for Scientific Computing (CSC) for providing the computational resources needed. T.K. would like to thank also the group members Karoliina Honkala and Atte Sillanpää for supportive and helpful discussions.

References

[1] P.M. Maitlis, A. Haynes, G.J. Sunley, M.J. Howard, J. Chem. Soc., Dalton Trans. (1996) 2187.
[2] D. Forster, J. Am. Chem. Soc. 98 (1976) 846.
[3] T.W. Dekleva, D. Forster, Adv. Catal. 34 (1986) 81.
[4] C.E. Hickey, P.M. Maitlis, J. Chem. Soc. Chem. Commun. (1984) 1609.
[5] A. Haynes, B.E. Mann, D.J. Gulliver, G.E. Morris, P. Maitlis, J. Am. Chem. Soc. 113 (1991) 8567.
[6] A. Haynes, B.E. Mann, G.E. Morris, P.M. Maitlis, J. Am. Chem. Soc. 115 (1993) 4093.
[7] T.R. Griffin, D.B. Cook, A. Haynes, J.M. Pearson, D. Monti, G.E. Morris, J. Am. Chem. Soc. 118 (1996) 3029.
[8] M. Cheong, R. Schmid, T. Ziegler, Organometallics 19 (2000) 1973.
[9] T. Kinnunen, K. Laasonen, J. Mol. Struct. (Theochem) 540 (2001) 91.
[10] F.E. Paulik, J.F. Roth, Chem. Commun. (1968) 1578.
[11] D. Forster, J. Chem. Soc., Dalton Trans. (1979) 1639.
[12] R.T. Eby, T.C. Singleton, Applied Industrial Catalysis, vol. 1 1983 (chap. 10).
[13] A.D. Becke, J. Chem. Phys. 98 (1993) 5648.
[14] C. Lee, W. Yang, R.G. Parr, Phys. Rev. B 37 (1988) 785.
[15] M.J. Frisch, G.W. Trucks, H.B. Schlegel, G.E. Scuseria, M.A. Robb, J.R. Cheeseman, V.G. Zakrzewski, J.A. Montgomery, R.E. Stratmann, J.C. Burant, S. Dapprich, J.M. Millam, A.D. Daniels, K.N. Kudin, M.C. Strain, O. Farkas, J. Tomasi, V. Barone, M. Cossi, R. Cammi, B. Mennucci, C. Pomelli, C. Adamo, S. Clifford, J. Ochterski, G.A. Petersson, P.Y. Ayala, Q. Cui, K. Morokuma, D.K. Malick, A.D. Rabuck, K. Raghavachari, J.B. Foresman, J. Cioslowski, J.V. Ortiz, B.B. Stefanov, G. Liu, A. Liashenko, P. Piskorz, I. Komaromi, R. Gomperts, R.L. Martin, D.J. Fox,, T. Keith, M.A. Al Laham, C.Y. Peng, A. Nanayakkara, C. Gonzalez, M. Challacombe, P.M.W. Gill, B.G. Johnson, W. Chen, M.W. Wong, J.L. Andres, M. Head-Gordon, E.S. Replogle, J.A. Pople, GAUSSIAN 98 (Revision A.3), Gaussian, Inc., Pittsburgh, PA, 1998.
[16] K. Mylvaganam, G.B. Bacskay, N.S. Hush, J. Am. Chem. Soc. 122 (2000) 2041.
[17] K. Mylvaganam, G.B. Bacskay, N.S. Hush, J. Am. Chem. Soc. 121 (1999) 4633.
[18] D. Forster, J. Am. Chem. Soc. 97 (1975) 951.
[19] R.J. Cross, Chem. Soc. Rev. 14 (1985) 197.
[20] J.M. Pearson, A. Haynes, G.E. Morris, G.J. Sunley, P.M. Maitlis, J. Chem. Soc., Chem. Commun. (1995) 1045.
[21] T.W. Dekleva, D. Forster, J. Am. Chem. Soc. 107 (1985) 3565.
[22] T. Ghaffar, H. Adams, P.M. Maitlis, G.J. Sunley, M.J. Baker, A. Haynes, Chem. Commun. (1998) 1023.